Fragility Functions for Eccentrically Braced Steel Frame Structures

Gerard J. O'Reilly[*1] and Timothy J. Sullivan[2]

[1]*ROSE Programme, UME School, IUSS Pavia, Italy*
[2]*Department of Civil Engineering and Architecture, University of Pavia, Italy*
(Received , Revised , Accepted)

Abstract. Eccentrically braced frames (EBFs) represent an attractive lateral load resisting steel system to be used in areas of high seismicity. In order to assess the likely damage for a given intensity of ground shaking, fragility functions can be used to identify the probability of exceeding a certain damage limit-state, given a certain response of a structure. This paper focuses on developing a set of fragility functions for EBF structures, considering that damage can be directly linked to the interstorey drift demand at each storey. This is done by performing a Monte Carlo Simulation of an analytical expression for the drift capacity of an EBF, where each term of the expression relies on either experimental testing results or mechanics-based reasoning. The analysis provides a set of fragility functions that can be used for three damage limit-states: concrete slab repair, damage requiring heat straightening of the link and damage requiring link replacement. Depending on the level of detail known about the EBF structure, in terms of its link section size, link length and storey number within a structure, the resulting fragility function can be refined and its associated dispersion reduced. This is done by using an analytical expression to estimate the median value of interstorey drift, which can be used in conjunction with an informed assumption of dispersion, or alternatively by using a MATLAB based tool that calculates the median and dispersion for each damage limit-state for a given set of user specified inputs about the EBF. However, a set of general fragility functions is also provided to enable quick assessment of the seismic performance of EBF structures at a regional scale.

Keywords: eccentrically-braced frame; fragility functions; steel; performance-based design; seismic assessment

1 Introduction

Seismic assessment of structures in terms of economic loss and downtime typically aims to relate the probability of a certain damage state with the seismic response of the structure through the use of fragility functions. These damage states can then be related to a cost of repair for that damage state and an associated repair time to give an estimation of the structure's economic loss and downtime. Fragility functions for different types of structures may be determined based on experimental testing, numerical analyses or by engineering judgement in the absence of test data (FEMA P58-1 2012).

For eccentrically braced frame (EBF) structures, such as that shown in Figure 1, Gulec *et al.* (2011) report test data from 110 different experimental tests on EBF links available in the literature and compile a database relating the occurrence of different damage limit-states to a

[1] ∗Corresponding author, Ph.D. Student, E-mail: gerard.oreilly@iusspavia.it
[2] Professor, E-mail: tim.sullivan@unipv.it

plastic chord rotation, which was chosen as the engineering demand parameter (EDP). However, since the link plastic chord rotation is a demand parameter not typically utilised in current assessment software, such as the Performance Assessment Calculation Tool (PACT) software (FEMA P58-1 2012; FEMA P58-2 2012), this set of fragility functions for EBFs creates difficulty in terms of its ease of application. Typically, EDP's such as interstorey drift and floor accelerations are used when performing a seismic assessment using software tools such as PACT, which represents the current state-of-the art in seismic assessment. As such, the goal of this paper is to develop a set of fragility functions for EBFs, which are based on interstorey drift as opposed to link plastic chord rotation, which can be quite tedious to establish whereas interstorey drift is a parameter engineers are more familiar with and already use in seismic assessment. From this, the user will be able to use a set of fragility functions for EBF structures in terms of the more familiar EDP interstorey drift, in addition to doing away with the need to separate the link demand in terms of its elastic and plastic components. It will be also shown by using the approach outlined here, a set of fragility functions can be derived for an EBF structure with just information about structural geometry, given certain simplifications. This latter approach represents a useful tool when conducting a more general and regional assessment of EBF structures.

This paper first examines the behaviour of EBFs by reviewing the expressions needed to calculate the yield interstorey drift of a single storey within an EBF system. Advanced numerical analyses are then used to illustrate the validity of the yield drift expression. Existing EBF fragility curves are discussed and the basis for the development of the interstorey drift-dependant fragility functions is then presented. This paper finally presents the analysis results and proposed fragility functions and demonstrates the application of each of these through example.

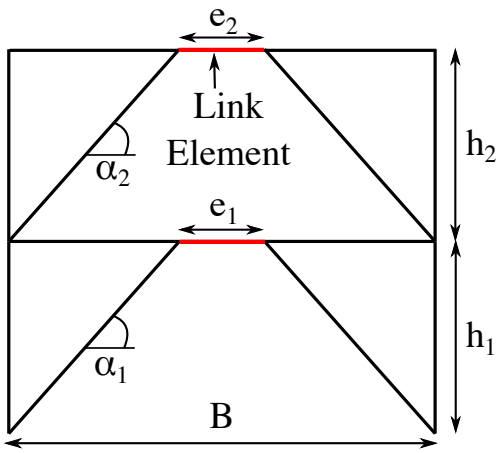

Figure 1: Typical layout of an EBF.

2 Characterising the Behaviour of Eccentrically Braced Frame Structures

EBF structures resist intense seismic loading through the inelastic deformation of a link element, such as that shown in Figure 1, which can be classified as either a short or long link through the ratio ρ, which is defined as:

$$\rho = \frac{e}{M_p / V_p} \qquad \textbf{Equation 1}$$

where e is the link length as per Figure 1, M_p and V_p are the plastic moment and shear capacities of the link section, respectively. A ρ value of 1.6 or less indicate a short link which yields primarily in shear as defined in numerous design codes such as AISC 341-10, CSA S16-09, Eurocode 8 and NZS 3404, whereas a ρ value greater than 3.0 indicates a long link which yields primarily in flexure, according the European and New Zealand standard, whereas the US and Canadian standards define a slightly lower value of 2.6. Link with values of ρ between these limits are expected to develop a combined flexure shear response.

In order to relate the interstorey drift demand with the likelihood of exceeding a certain damage state in an EBF structure, one requires expressions for both the elastic (yield) interstorey drift and plastic interstorey drift capacity, which summed together to give the total interstorey drift capacity. This section first presents an expression for the yield drift of EBF systems proposed by Sullivan (2013) which is reviewed and existing relationships for the plastic drift capacity relating the link chord rotation demand to the interstorey drift demand are combined to arrive at an estimate of the total drift capacity.

2.1 EBF Yield Drift Expression

As explained in Sullivan (2013), the yield drift of an EBF structure is principally composed of three deformation components:

1. Beam (including link) bending and shear deformation.
2. Brace axial deformation.
3. Column axial deformation.

This section presents simplified expressions to calculate each of these three components and in turn, the yield drift of an individual storey in an EBF structure consisting of a single bay with a single central link element, as illustrated in Figure 1. This yield drift relationship is then compared to values obtained from an experimentally validated numerical model of various configurations of an EBF structure.

2.1.1 Beam Deformation Component

An expression to describe the vertical displacement of a single beam section at the end of each link due to vertical shear forces developed in the link during loading is described in Mazzolani *et al.* (2006) and is elaborated in Sullivan (2013) to give an expression which gives the interstorey drift at the point of yielding in the links. One of the assumptions is that the beam cross-section remains the same for regions both outside and within the link section of the beam. This implies that in order to use systems such as those discussed in Mansour (2010), which may comprise of removable links with different cross sections to the surrounding beam elements, the following expressions would need to be adjusted. The resulting expression for the drift contribution due to link deformation of a given storey i, depicted in Figure 2(a), is given in Sullivan (2013) by:

$$\theta_{link,i} = \frac{f_y A_{v,i} e_i}{\sqrt{3}(B - e_i)} \left(\frac{e_i (B - e_i)}{12 E I_{zz,i}} + \frac{1}{G A_{v,i}} \right) \qquad \textbf{Equation 2}$$

where the general notation is as illustrated in Figure 2(a), with I_{zz} representing the second moment of area of the beam about the major axis, f_y is the steel yield strength, E and G are the elastic and shear moduli of steel, respectively. The shear area (A_v) is taken to be the product of the entire height of the section (h) times the web thickness (t_w) as recommended by Della Corte *et al.* (2013), which concluded that this represents the best estimate of shear area of European HE link sections compared to the expression given in Eurocode 3 (EN 1993-1-1:2005 2005) when comparing the shear stiffness of both expressions to values obtained from finite element analyses.

2.1.2 Brace Deformation Component

The expression describing the deformation contribution due to the axial elongation of the brace elements depicted in Figure 2(b) is given in Sullivan (2013) as:

$$\theta_{br,i} = \frac{2k_{br,i}\varepsilon_y}{\sin(2\alpha_i)} \qquad \textbf{Equation 3}$$

where ε_y is steel yield strain, α is the brace angle and $k_{br,i}$ represents the brace strain ratio, which can be computed as the ratio of the seismic design axial force, $N_{Ed,br,i}$, to the brace section yield force, $N_{c,Rd,br,i}$:

$$k_{br,i} = \frac{N_{Ed,br,i}}{N_{c,Rd,br,i}} \qquad \textbf{Equation 4}$$

where the terms $N_{Ed,br}$ and $N_{c,Rd,br}$ represent the design action and capacity axial forces of the brace section, respectively, where the axial capacity is the full section compression capacity (i.e. Af_y) and is not to be confused with the buckling capacity of the member. The product of $k_{br,i}$ with ε_y gives the expected axial strain in the brace at yield of the link and therefore, knowing the brace strain and length, the brace contribution to the interstorey drift can be found.

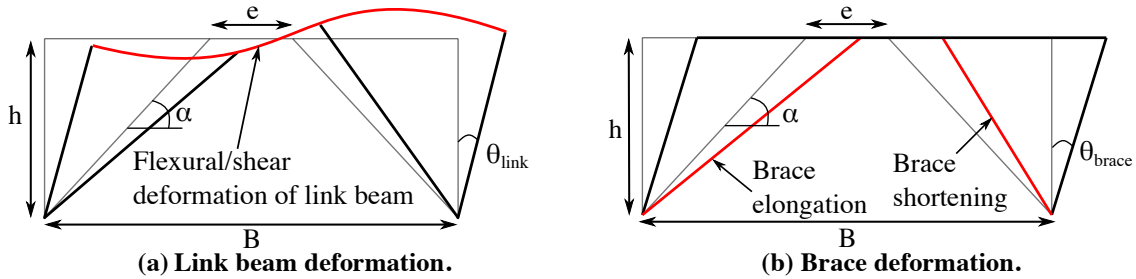

(a) Link beam deformation. **(b) Brace deformation.**

Figure 2: Link and brace deformation components.

2.1.3 Column Deformation Component

For a given storey in a multi-storey building, the axial deformations of the columns in the lower storeys lead to the development of a rigid body rotation of the storeys above. This contribution is calculated in much the same way as the brace elongation contribution, where the ratio of the design force to the section yield force is used to provide an estimate of the expected column strain, which can then be converted into an equivalent rigid body rotation of the storey, as depicted in Figure 3(a). This is given by:

$$\theta_{col,i} = \frac{2k_{col,i-1}\varepsilon_y H_{i-1}}{B} \qquad \textbf{Equation 5}$$

where H_{i-1} is the elevation of the floor below the one being considered and $k_{col,i-1}$ represents the average column strain ratio. As there can be many storeys below the storey i being considered, there are many ratios of design to capacity axial load ratios. The average value of these is therefore used in the expression, which is thus calculated by:

$$k_{col,i-1} = \frac{1}{i-1}\sum_{j=1}^{i-1}\frac{N_{Ed,col,j}}{N_{c,Rd,col,j}} \qquad \textbf{Equation 6}$$

where $N_{Ed,col}$ represents the design axial force on the column member and $N_{c,Rd,col}$ the full compressive capacity of the column section, again not to be confused with the member buckling capacity.

In addition to the axial deformations of the storeys below the one being considered, there is also the contribution of the axial deformations of the storey in question, which is shown in Figure 3(b). The contribution of this deformation mode is noted in Sullivan (2013), where it was proposed to simply ignore it, as it is difficult to incorporate into the expression in Equation 5, and also because the exclusion of this term gave reasonably accurate results in any case. For a given storey, this additional deformation due to the axial elongation and shortening of the storey's column is derived as follows:

$$\theta_{col,axial,i} = \frac{1}{h_i}\sqrt{\left(\frac{B-e_i}{2}\right)^2 + h_i^2 - \left(h_i - \frac{\overline{V}_i e_i h_i}{BEA_{col,i}}\right)^2} - \frac{1}{\tan\alpha_i} \qquad \textbf{Equation 7}$$

where h_i is the individual storey height and $A_{col,i}$ is the cross-sectional area of the column.

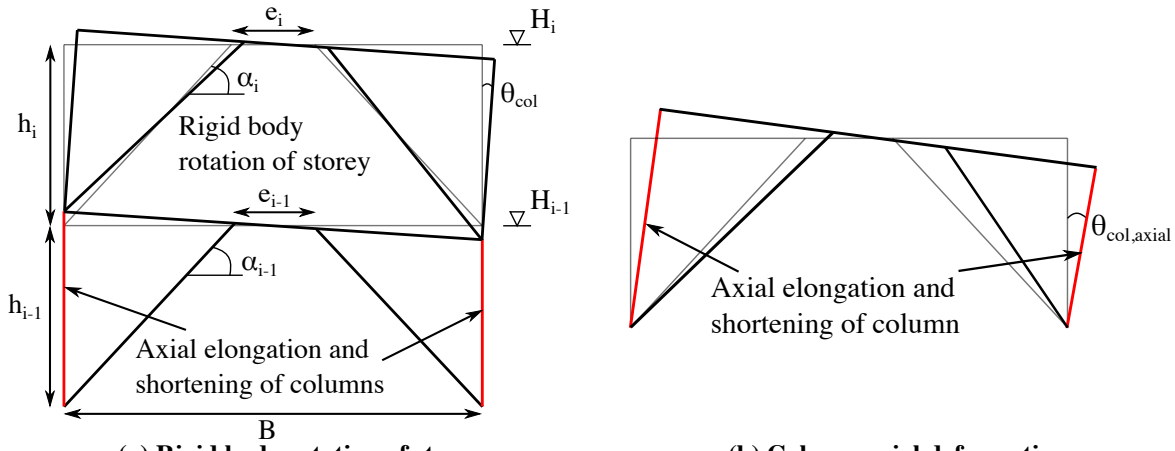

(a) Rigid body rotation of storey. **(b) Column axial deformation.**

Figure 3: Column deformation components.

Figure 4 shows the relative contributions of each of the link deformation, brace deformation, rigid body rotation due to axial deformations of lower columns and the drift contribution due to the axial deformations of the given storey for a variety of EBF structures. These yield drift

contributions represent the yield drift contributions at the roof level of each of the soil type C designs outlined in O'Reilly and Sullivan (2015) which consisted of uniform storey heights of 3.5m, bay width of 7m and S450 grade steel. These structures were all designed to a Eurocode 8 (EN 1998-1:2004 2004) response spectrum for a soil type C site which has an equivalent PGA on soil type A of 0.4g. It can be seen from Figure 4 that the relative contribution of the column's axial deformations is quite small (less than 2% of the total yield drift), which confirms the remarks by Sullivan (2013) that it has relatively little contribution to the overall interstorey drift and can be ignored, given its lengthy expression.

Combining Equations 2, 3 and 5, the total storey drift at yield of a single storey within an EBF structure can be computed:

$$\theta_{y,i} = \theta_{link,i} + \theta_{br,i} + \theta_{col,i} = \frac{\overline{V}_i e_i}{B - e_i}\left(\frac{e_i(B-e_i)}{12EI_{zz,i}} + \frac{1}{GA_{v,i}}\right) + \frac{2k_{br,i}\varepsilon_y}{\sin(2\alpha_i)} + \frac{2k_{col,i-1}\varepsilon_y H_{i-1}}{B} \quad \textbf{Equation 8}$$

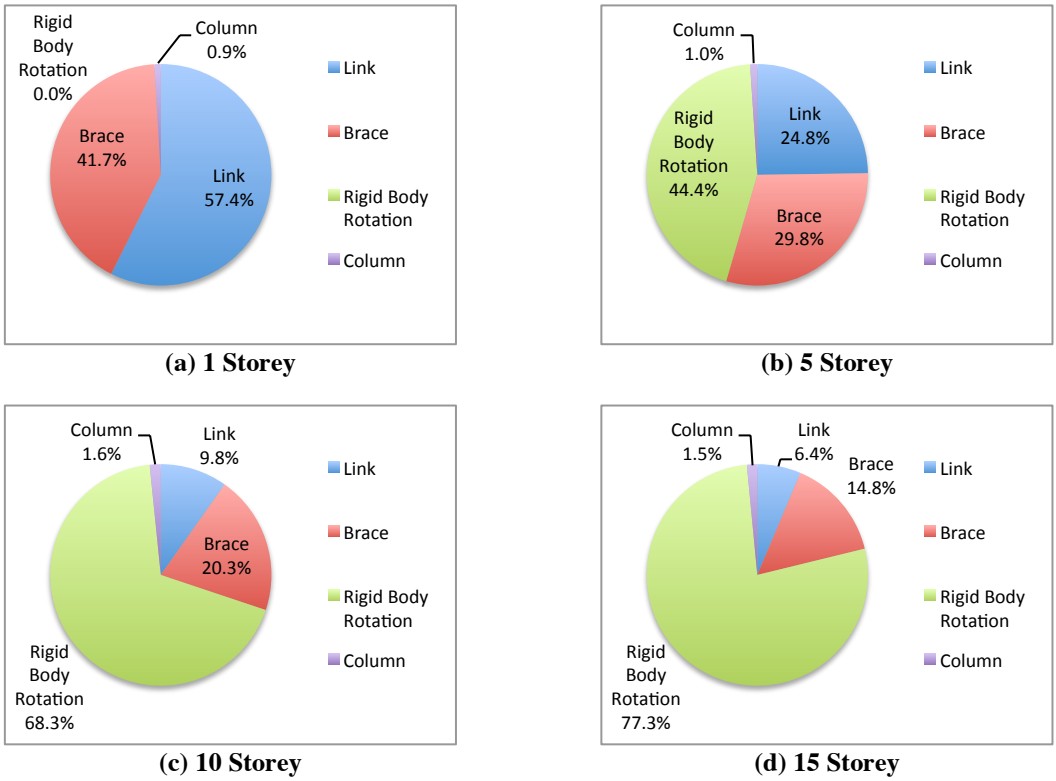

Figure 4: Yield drift contribution of each of the deformation components.

2.2 *Verification of Yield Drift Expression for EBFs*

The yield drift expression given by Equation 8 can be compared with results obtained from a numerical model to gauge its accuracy and validate its use later in this study. Hence, the validation

of expressions describing the yield drift of a range of EBFs is required to proceed with confidence. A total of 112 variations of the EBF model were analysed from pushover analysis using OpenSees (McKenna et al. 2000). The variations consisted of EBFs with a constant storey height of 3.5m, bay width of 7M and grade S355 steel. Section sizes were varied between HE160B and HE650M of the European section size catalogue (Corus 2006), where for each section size, the link length was determined as 40, 50 and 60% of the maximum link length in order to remain classified as a link length, which is found by rearranging the expression in Equation 1. The model, illustrated in Figure 5, consists of a force-based beam-column element for the modelling of the link elements in axial and flexural behaviour with an uncoupled shear hinge added to the link element to model the nonlinear shear behaviour expected in short links. Brace elements have been modelled as elastic truss elements with pinned end connections. Column members have also been modelled as elastic elements as these, along with the braces, are expected to remain elastic throughout nonlinear response. In addition, the connection between the beams and the columns is modelled as a pinned connection, as shown in Figure 5. In addition, a comparison between the link shear behaviour predicted by the proposed OpenSees model with a specimen tested by Mansour (2010) is also shown in Figure 5, where an excellent match between the numerical model and the experimental response both in terms of the link capacity and hysteretic behaviour can be observed. Since the purpose of using such a model in this study is to evaluate the expression derived for the yield drift of the EBF configuration, no fracture criterion has been considered, although such a model may be adopted in the future to include such considerations either by introduction of an upper limit on the deformation capacity through the use the MaxMin material model available in OpenSees, or through the introduction low-cycle fatigue similar to that developed by Uriz and Mahin (2008) for concentrically braced steel frames by utilising experimental testing and observations by Okazaki et al. (2005) for example, but such work is deemed beyond the scope of this paper. Further detailing on the modelling and its calibration can be found in the original publication by O'Reilly and Sullivan (2015).

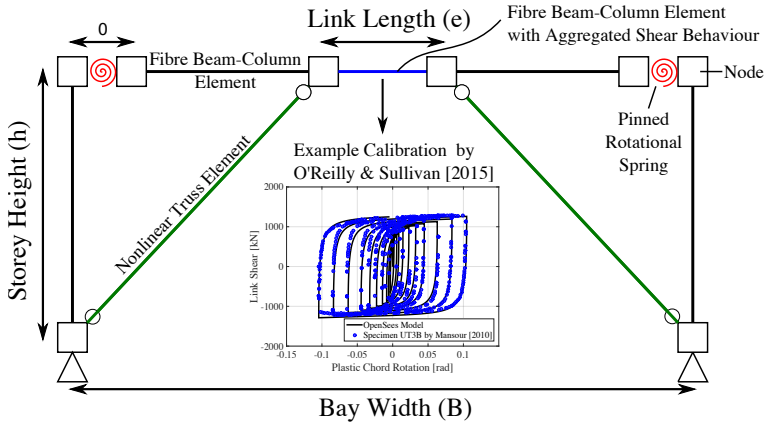

Figure 5: Illustration of EBF model proposed by O'Reilly and Sullivan (2015).

From these pushover analyses performed on existing designs of EBFs, the yield drift was determined and compared to what is given by Equation 8 in each case. A comparison of these two sets of data is shown in Figure 6, where the predicted yield drift is plotted against the observed

numerical drift. As is evident from Figure 6, Equation 8 predicts the yield drifts well and is deemed to be sufficient for later use in conjunction with an expression for plastic drift to give the total drift capacity of a single storey, which is discussed further in Sections 2.4 and 2.5.

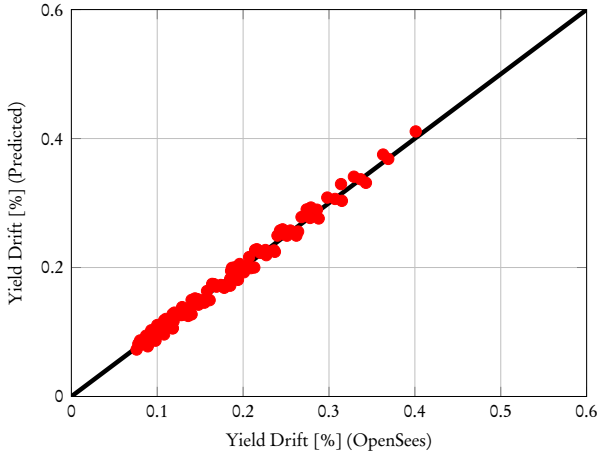

Figure 6: Predicted versus observed yield drift.

2.3 EBF Yield Drift Parameter Sensitivity

The expression developed for the yield drift of an EBF in Section 2.1 consists of a number of terms relating to the geometry and member properties of an EBF. In order to evaluate the sensitivity of the yield drift to these individual parameters, a parametric study is conducted in order to establish the principle parameters that contribute to the variation of yield drift for a given reference configuration. This reference configuration is taken as a HE280B section for links and columns with a 600mm link length at the fifth storey in a structure. The brace and column strain ratios (Equations 4 & 6) are taken as 0.3 and 0.4, respectively, which are deemed reasonable values noting that the ratio is usually significantly less than 1.0 as a result of differences between member buckling and resistance and the section resistance used in Equations 4 and 6. The values varied in this study are given in Table 1 together with the relevant justifications, which are based on engineering judgement.

Table 1: Sensitivity study parameter range.

Parameter		Range	Step	Unit	Justification
Link length	e	300-1400	100	mm	Upper limit in order to maintain $\rho < 1.6$
Bay width	B	5-12	0.5	m	Reasonable range of bay widths.
Storey height	h	3-5	0.5	m	Reasonable range of storey heights.
Number of storeys	n	1-10	1	-	Reasonable range of storeys.
Link shear area	A_v	640-6750	-	mm^2	HE140B to HE550A section sizes.
Yield strength	f_y	235-450	-	MPa	Grades S235, S275, S355 and S450 steel.

Computing the yield drift from Equation 8 for the range of parameters listed in Table 1 which are normalised by the reference configuration described above, the influence of different parameters

on the yield drift normalised by the yield drift of the reference configuration are given in Figure 7, where it can be seen that the influence on yield drift varies greatly between parameters. It can be seen that the parameters that the yield drift is most sensitive to are the number of storeys, where the elastic rigid body rotation of the storeys below increases as the number of storeys increases, steel yield strength and bay width. In addition to these, it can be seen that the storey height has minimal influence on the yield drift of the storey, hence it is deemed to be insensitive to these parameters and this is not considered in the drift capacity fragility analysis discussed in Section 3.

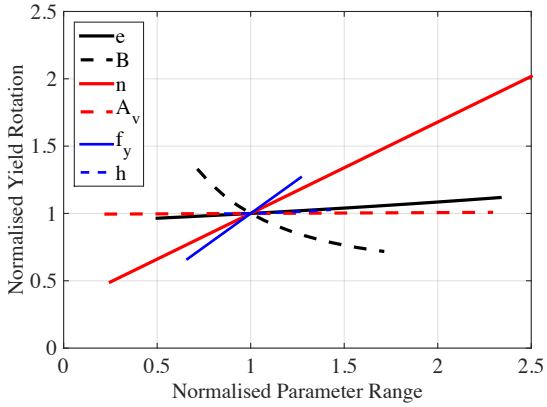

Figure 7: Normalised yield drift sensitivity.

2.4 EBF Plastic Drift Capacity

Experimental testing by Engelhardt and Popov (1989) at the University of California, Berkeley in the 1980's reported the deformation capacity of the links in terms of the plastic chord rotation (γ_p), where the elastic component rotation was removed. For short links, (Engelhardt and Popov 1989) proposed 0.08rad for the design plastic rotation of short links, which were defined as the deformations for which a well-detailed link was able to provide stable hysteresis. These design limits for plastic chord rotation appear to have been subsequently adopted in design codes such as Eurocode 8 (EN 1998-1:2004 2004), AISC 341-10 (AISC 341-10 2010), CSA S16-09 (CSA S16-09 2009) and NZS 3404 (NZS 3404 2007).

In order to define the plastic storey drift capacity, these limits need to be related to an interstorey drift, which is given by:

$$\theta_{p,i} = \frac{e_i \gamma_p}{B} \qquad \textbf{Equation 9}$$

In addition to the experimental data from Engelhardt and Popov (1989), which appears to have been subsequently adopted by most design codes, Gulec *et al.* (2011) collects data from 110 different tests, including more recent testing at the University of Texas, Austin (Arce 2002; Galvez 2004; Okazaki and Engelhardt 2007; Ryu 2005), which uses the testing protocol proposed by Richards and Uang (2006) and subsequently adopted by AISC 341-10 (AISC 341-10 2010) that considers the accumulation of damage in the links for each cycle and compares this to what is

typically observed in nonlinear dynamic analysis of EBF structures using real earthquake ground motion records. Therefore, this loading protocol is more representative of the damage accumulation to EBF links to be expected during an earthquake, which has been noted to have a direct impact on the plastic chord rotation capacity (Kuşyilmaz and Topkaya 2015). Gulec *et al.* (2011) compiles this experimental data and provides a set of limit-state fragility functions for EBF links. These limit-state fragility functions can be integrated into an expression for interstorey drift, such as Equation 10, in the same way the design code prescribed values are. However, by using the values proposed by Gulec *et al.* (2011), the variability of the limit-state values is considered, which is then used in this study for the development of a interstorey drift-based fragility function as opposed to a plastic link rotation-based function. The advantage of using an interstorey drift-based fragility function is that this is more direct when assessing probabilities of exceeding certain limit-states as just the interstorey drift is required, as opposed to the plastic chord rotation demands, which needs to be separated from its elastic components, which can be a tedious task.

2.5 EBF Total Interstorey Drift Capacity Expression

In addition to the experimental data from the expression for the plastic drift capacity from Section 2.4 together with the yield drift expression from Section 2.1, the total drift capacity of a single storey of a short link EBF structure with a single bay and central link element is obtained from the sum of the two as:

$$\theta_{c,i} = \frac{f_y A_{v,i} e_i}{\sqrt{3}(B-e_i)}\left(\frac{e_i(B-e_i)}{12EI_{zz,i}} + \frac{1}{GA_{v,i}}\right) + \frac{2k_{br,i}\varepsilon_y}{\sin(2\alpha_i)} + \frac{2k_{col,i-1}\varepsilon_y H_{i-1}}{B} + \frac{e_i\gamma_p}{B} \qquad \textbf{Equation 10}$$

where the symbols have been defined earlier in Sections 2.1 and 2.4. It should be noted that the above expression is valid for an EBF system with a centrally placed link, as illustrated in Figure 1. Should the user require fragility functions for EBF systems with link elements located at one end, the above expressions would need to be revised to consider the different behaviour of such a system. As such, the fragility functions described in this article relate to EBF configurations such as in Figure 1, although the same approach could be adopted for other systems.

While it should be clear that this equation could provide a useful indication of the likely drift capacity of an EBF system, it is apparent that not all the data required to use the expression will always be available during the seismic assessment of a building or a group of buildings. For instance, in a regional assessment of the vulnerability of EBF systems one might only have information on the number of storeys and likely material properties of the EBFs. To this extent, the availability of fragility functions that are formulated as a function of various possible input parameters could be quite advantageous. The following sections will illustrate how such fragility functions can be established.

3 Development of Fragility Function for EBF Structures

Fragility functions describe the probability of exceeding a predefined damage limit-state given a certain value of EDP. Damage limit-states can be defined at a global level, such as serviceability or collapse, or on a local element level, such as link yielding or fracture. An EDP is a parameter associated with the magnitude of the response of the structure, where typical global EDP's are interstorey drift and floor accelerations and an example of a local EDP is element chord rotation.

3.1 Existing EBF Fragility Functions

As previously outlined in Section 2.5, Gulec *et al.* (2011) compiles experimental data from 110 tests documented in the literature to provide a set of damage limit-state fragility functions for EBF links. The damage limit-states are defined in terms of slab damage, link web and flange yielding, and local buckling and fracture observed during the experimental tests, and a set of fragility functions were derived based on these. Such fragility functions have been implemented in PACT (FEMA P58-1 2012), which is a software tool that performs a seismic performance assessment of structures given the building's dynamic response to earthquakes of ranging return periods. However, one drawback to using the fragility functions proposed in Gulec *et al.* (2011) is that the EDP is specified in terms of plastic link chord rotation (γ_p), as this is typically reported from experimental tests on EBF links. Typically, users input EDPs such as interstorey drift and floor accelerations into PACT for seismic performance assessment. This means that should a fragility function for EBFs be proposed with an EDP in terms of interstorey drift, this would simplify performance assessments as it would remove the need to extract the plastic component of the link element chord rotation demands from the results of structural analyses and would greatly assist loss assessment studies conducted using either a comprehensive approach (Porter 2003; FEMA P58-1 2012; FEMA P58-2 2012) or simplified methods (Porter, Beck, and Shaikhutdinov 2004; Welch, Sullivan, and Calvi 2014), as these types of EDPs are typically used in such loss assessment approaches.

3.2 Proposed Approach

In order to derive a set of fragility functions for EBF structures with interstorey drift as the EDP, the expression developed and validated in Section 2 is used in conjunction with distributions for the various parameters affecting storey drift, including to the distributions associated with the different damage limit-state distributions proposed by Gulec *et al.* (2011). Using the distributions of all of the various parameters, Monte Carlo Simulation (MCS) is used to sample values for each variable and calculate the interstorey drift capacity (θ_c) using Equation 10 to give a data set which describes the distribution of the interstorey drift capacity. Using this distribution of θ_c for a given damage state, a fragility function for an EBF is then derived in terms of interstorey drift, which can be directly used in current seismic performance assessment tools, such as PACT. Section 2.3 discussed the sensitivity of θ_y to the various parameters contained within the expression. Four of these; bay width (B), link length (e), number of storeys (n) and link shear area (A_v), are variables that heavily influence θ_c but are considered deterministic variables, as opposed to probabilistic variables with an associated distribution. As such, fragility functions are developed in terms of a specific combination of bay width, link length, storey number, link section and damage limit-state. It is important to acknowledge the sources of uncertainty that exist within the fragility functions developed using the proposed approach. Firstly, the aleatory uncertainty in the drift capacity is introduced via the dispersion in the test data reported by Gulec et al. (2011), since this dispersion represents the randomness in the drift capacity of EBF links seen in experimental testing. Secondly, an additional uncertainty known as epistemic uncertainty is introduced in the proposed approach as this reflects the uncertainty in knowing the actual drift capacity. However, for the various sets of fragility function sets discussed in Section 4, it will be shown that with increased knowledge of the EBF structure, the epistemic uncertainty can be reduced.

3.3 Probabilistic and Deterministic Distributions of Yield Drift Parameters

As discussed in Section 3.2, some of the variables used in the MCS of Equation 10 are assigned a distribution and some are assigned deterministic values. The values for storey height (h), elastic (E) and shear (G) moduli of steel are taken here to be 3.5m, 210GPa and 81GPa, respectively. These are kept constant throughout the analysis, as Equation 10 has been shown to be relatively insensitive to these terms. As for deterministic values, the link size and length, bay length and number of storeys are all deterministic values envisaged as known parameters by the user and are variables that do not constitute a distribution, but rather a predetermined range of values. This was conducted for EBF systems with a number of storeys between 1 and 15 and the entire European HEA, HEB and HEM section size catalogue (Corus 2006). Since short links are defined by a ratio ρ less than 1.6, which is a function of the link cross-section and link length, the maximum possible link length can be determined for a given section in order for it to still be classified as a short link by rearranging Equation 1. Therefore for each section, the maximum link length (e_{max}) in order to be still classified as a short link according to a rearranged Equation 1 was determined for each cross-section and four link lengths equal to 40%, 60%, 80% and 100% of e_{max} were used in the simulations. Bay widths were varied between 5 and 12m in increments of 1m.

Values for the yield strength of steel (f_y), link plastic chord rotation capacity (γ_p), brace axial load ratio (k_{br}) and average column axial load ratio (k_{col}) are all taken to be probabilistic values with an associated mean and dispersion. These values are listed in Table 2 along with the other values and their associated distributions. For the steel yield strength, experimental testing by Braconi *et al.* (2010) on European grade S355 steel is taken as the distribution for f_y, which is a normal distribution with a mean of 355MPa and standard deviation of 27MPa. For the axial load ratios of the braces (k_{br}) and columns (k_{col}), a series of pushovers of a total of 38 EBF structures presented in Rossi and Lombardo (2007) and O'Reilly and Sullivan (2015) has provided a set of values for buildings designed in that report, which allows a reasonable value of median and standard deviation to be estimated in both cases. Since a normal distribution is assumed for both the k_{br} and k_{col}, any samples that give values outside the range of 0 and 1 are removed from the simulation, as these do not represent physically possible scenarios.

The distributions of link plastic chord rotation capacity come from the data published by Gulec *et al.* (2011) for three limit-states identified from the test results and engineering judgement. These three damage limit-states corresponded to:

- Damage State 1 (DS1): plastic chord rotation resulting in concrete slab repair being required.
- Damage State 2 (DS2): plastic chord rotation for which heat straightening of the link is required.
- Damage State 3 (DS3): plastic chord rotation resulting in complete link replacement being required.

These values are given as lognormal distributions by Gulec *et al.* (2011) and their associated values are given in Table 2. The link stiffener spacing considered was such that the links used in the dataset satisfied the AISC 341-10 maximum link stiffener spacing of $30t_w$-d/5, where t_w is the web thickness of the link section and d is the depth of the section. In addition, some uncertainty associated with the data presented in Gulec *et al.* (2011) arises from the effects of loading protocol on the link capacity, where depending on the loading history to test the link member, different

plastic rotation capacities can be observed. This was highlighted by Richards and Uang (2006) where it was concluded that the loading protocol used by researchers at the University of California, Berkeley such as Engelhardt and Popov (1989) was too severe and the actual plastic chord rotation capacity ought to be a little higher than reported from those tests if a different loading protocol was used. Further testing by Okazaki *et al.* (2009) at the University of Texas using a revised loading protocol for short links showed a slightly larger plastic chord rotation capacity of the links. Data from both tests has been included in the dataset used in Gulec *et al.* (2011) and no distinction is made between different loading protocols, which is acknowledged here as a source of uncertainty.

Table 2: Random variable distribution models and associated values.

Parameter		Unit	Distribution Model	Median	Dispersion
Link length	e	m	Deterministic	-	-
Number of storeys	n	-	Deterministic	-	-
Link shear area	A_v	mm^2	Deterministic	-	-
Bay width	B	m	Deterministic	-	-
Yield strength	f_y	MPa	Normal	355	27
Brace axial load ratio	k_{br}	-	Normal	0.3	0.1
Column axial load ratio	k_{col}	-	Normal	0.4	0.1
Link plastic chord rotation	γ_p (DS1)	rad	Lognormal	0.040	0.30
Link plastic chord rotation	γ_p (DS2)	rad	Lognormal	0.056	0.30
Link plastic chord rotation	γ_p (DS3)	rad	Lognormal	0.076	0.34

3.4 Analysis and Results

The MCS of the parameters outlined in Table 2 using Equation 10 yielded over 5000 simulations, where 1000 values were sampled for each of the random variables listed in Table 2. Each of these simulations were tested using the Lilliefors goodness-of-fit test at the 5% significance level (Ang and Tang 2007), which were tested against the null hypothesis that the interstorey drift capacity was of a lognormal distribution. Each simulation returned the result that the null hypothesis could not be rejected at the 5% significance level. An example of the results of such a simulation is shown in Figure 8, where the simulated data is shown alongside its fitted lognormal distribution. The plot of observed distribution of the interstorey drift capacity data from the MCS versus that predicted by the fitted distribution shows a one-to-one plot of the comparison between the data's cumulative distribution function and the fitted lognormal distribution. The simulated data from the MCS was fitted to a lognormal using the method of moments (Ang and Tang 2007), where the median and dispersion for the simulated data was fitted to the corresponding lognormal distribution given the Lilliefors test acceptance.

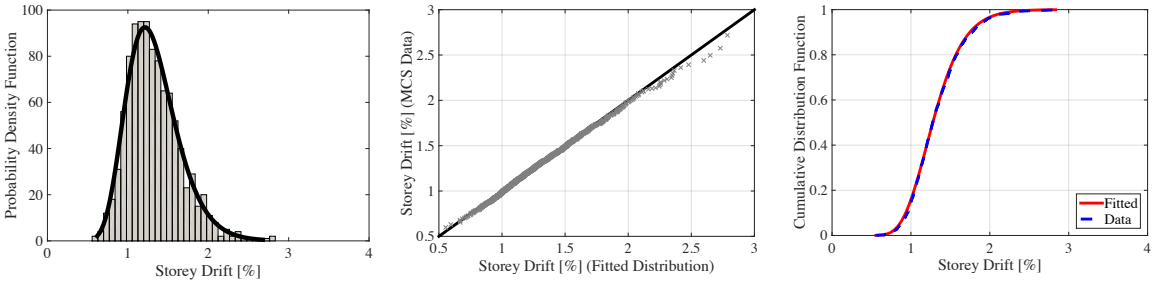

(a) Probability distribution **(b) 1 to 1 plot** **(c) Cumulative distribution**

Figure 8: Simulation results example (HE260B, n=5, e=0.781m, B=7m, DS3).

4 Proposed Fragility Function for EBF Structures

4.1 Overview

For each of the damage limit-states, the individual cumulative distribution functions (CDF's) for each simulation are reported in the following three ways:

1. Generic EBF Fragility: The fragility functions for each of the damage limit-states are reported that do not need specification of any details, and are hence termed the general fragility function set. This set considers all of the different link section sizes, link lengths, bay widths and storey numbers simulated in the dataset and hence the dispersion associated with this fragility function set is relatively large as a result. Since this is a more global fragility curve set, it can be used to assess the performance of the EBF structures on a more regional scale without actually knowing many details about the structures.
2. Storey Specific EBF Fragility: A storey specific set of fragility functions is presented, where the storey number being considered within a structure is specified to reduce the dispersion in the general fragility set. This specification of terms could be equally done for link length or section size, but given the rigid body rotation's prominence in yield drift contribution to higher storey buildings shown in Figure 4, a refinement in terms of the storey number only was carried out also considering that the storey number is an easy parameter to determine in building assessment.
3. Refined EBF Fragility: Since the MCS performed to generate these fragility function sets was performed using Equation 10 with the relevant distributions of the variables outlined in Table 2, it is proposed that this expression can be used directly to determine a median drift by just specifying the median values of the input parameters for a given case. The dispersion associated with this median could then be approximated based off of the observed dispersion of the MCS results. This approach has the advantage of giving the user more control for the specification of parameters, while simplifying the probabilistic side through the adoption of a reasonable dispersion based on the results of more thorough analysis.

Lastly, the code used to perform the MCS of the data is converted into a MATLAB (MATLAB 2014) based function, where the user can specify the details of the building directly and receive a set of fragility functions for that specific case through the MCS method outlined above. These four approaches are then compared for an example storey in a structure to demonstrate their

applicability and how they can be used to perform a quick general assessment or a more detailed assessment, depending on the level of detail known about an EBF structure.

4.2 Generic EBF Fragility Function

Should a general set of fragility functions irrespective of link section size, link length, bay width and number of storeys be required for general or regional assessment, Table 3 shows the values for the three limit-states considered, where Figure 9 shows the plot of these fragility functions along with the individual fragility functions used to generate them from each MCS and are plotted together in Figure 10.

Table 3: Mean and dispersion for a general fragility function.

	$\hat{\theta}$ [%]	β
DS1	1.04	0.48
DS2	1.23	0.48
DS3	1.48	0.49

As can be seen from Figure 9, the range of the fragility functions is quite wide although for individual curves, the dispersion is quite low but the general combined function is quite disperse reflecting the wide range of fragility functions for each MCS considered.

4.3 Storey Specific EBF Fragility Function

Should the storey number (i) within a structure be known, the fragility function set shown in Figure 10 can be refined further, which will reduce the associated dispersion for these damage limit-states. Table 4 shows the median and dispersion for up to fifteen storeys, which were considered in the analysis for each limit-state. As such, if one were interested in the fragility at DS3 of the 4th floor of an EBF structure, possessing a total number of storeys anywhere between 4 and 15 storeys, then from Table 4 they would estimate the median drift capacity of 1.38% and a dispersion of 0.42. As expected, the median drift increases between damage limit-state and also with increasing height due to the increase in the contribution of the rigid body rotation as a result of the axial shortening of the columns in the lower storeys. It is also noticed that the dispersion of the values is greatly decreased with respect to the general set shown in Table 3 and Figure 10, where the storey number was not specified. This highlights how the dispersion of the fragility function sets can be reduced should more details be known about the structure. It is also worth noting that the dispersion associated with the data decreases as one increases the storey number of the structure. That is, if the fragility function set of the first level of a structure is compared to what would be used for the fifteenth level of the structure; the dispersion is much less at the fifteenth level's than at the first. This is because as the storey number increases, so too does the contribution of the rigid body rotation of the lower storeys to the interstorey drift capacity, as was seen in Figure 4. The main variables associated with this contribution are the terms k_{col} and f_y, and the corresponding standard deviation's of these terms are quite low in comparison to others in Equation 10, thus providing reason that as this term with a relatively low dispersion becomes more prominent, the overall dispersion is to decrease.

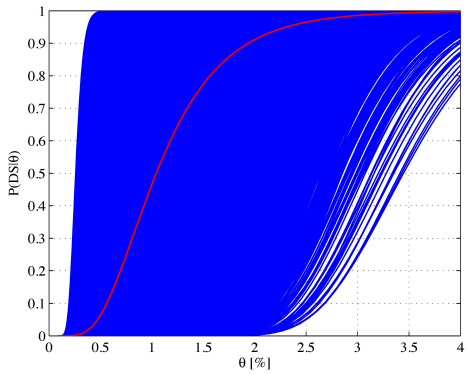

(a) DS1

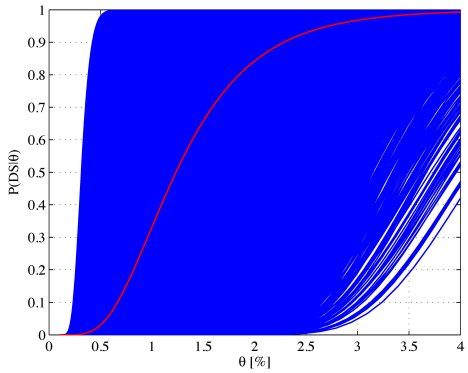

(b) DS2

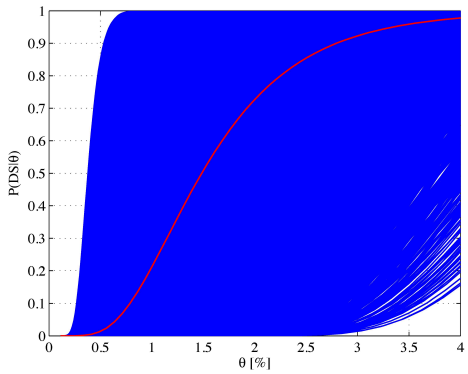

(c) DS3

Figure 9: General EBF fragility functions.

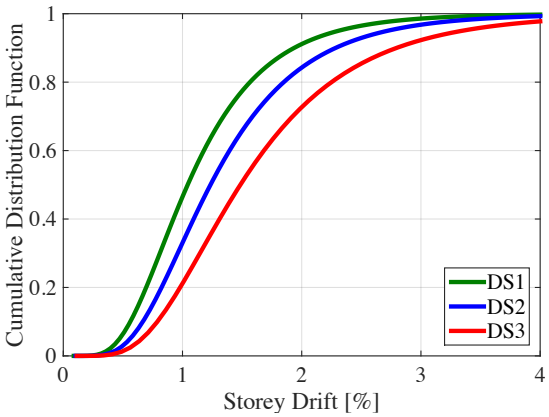

Figure 10: Proposed EBF fragility functions.

Table 4: Median and dispersion for a storey-based fragility function.

	DS1		DS2		DS3	
i	$\hat{\theta}$ [%]	β	$\hat{\theta}$ [%]	β	$\hat{\theta}$ [%]	β
1	0.68	0.44	0.89	0.46	1.17	0.49
2	0.75	0.40	0.96	0.42	1.24	0.46
3	0.81	0.37	1.03	0.39	1.31	0.44
4	0.88	0.34	1.10	0.37	1.38	0.42
5	0.95	0.32	1.16	0.36	1.44	0.40
6	1.02	0.31	1.23	0.34	1.51	0.38
7	1.08	0.30	1.30	0.33	1.58	0.37
8	1.15	0.29	1.37	0.32	1.65	0.36
9	1.22	0.28	1.43	0.31	1.72	0.35
10	1.29	0.27	1.50	0.30	1.78	0.34
11	1.35	0.27	1.57	0.29	1.85	0.33
12	1.42	0.26	1.64	0.28	1.92	0.32
13	1.49	0.26	1.70	0.28	1.99	0.31
14	1.56	0.25	1.77	0.27	2.05	0.31
15	1.62	0.25	1.84	0.27	2.12	0.30

4.4 Refined EBF Fragility Function

As mentioned previously, it is also proposed to use the drift capacity relationship outlined in Equation 10 for the direct calculation of a median interstorey drift capacity, followed by an assumption for the associated dispersion. This allows for the direct calculation of median interstorey drift values using the information regarding link dimensions, storey number and bay width. Equation 10 is rewritten in a more simplified form with the inclusion of some terms in Table 2 to allow easier use when inputting the basic variables required. This way only the link dimensions (A_v, e, I_{zz}), storey number within the structure (i), steel grade (f_y, E, G), bay length (B) and are required to give the median value of drift capacity for a given damage limit-state (γ_p(DS)):

$$\hat{\theta}_{c,i} = \frac{f_y A_{v,i} e_i}{\sqrt{3}(B-e_i)}\left(\frac{e_i(B-e_i)}{12EI_{zz,i}} + \frac{1}{GA_{v,i}}\right) + \frac{0.6f_y}{E\sin\left(2\arctan\frac{2h_i}{B-e_i}\right)} + \frac{0.6f_y h_i(i-1)}{BE} + \frac{e_i\gamma_p(DS)}{B} \qquad \textbf{Equation 11}$$

Using this in conjunction with an assumed dispersion based on results of the MCS, a set of fragility functions can be formed rather easily. Appropriate values to be assumed for this dispersion are found from examination of the values observed from the Monte Carlo Simulation for each damage state. Collecting the dispersion values for each of the damage states, Figure 11 shows the corresponding dispersion versus median drift capacity for each of the damage states. From this, there is a trend in the increase of the dispersion values between damage states. Using Figure 11 as an indication of appropriate values for the anticipated dispersion values to be used in conjunction with Equation 11, the average values shown in Figure 11 are proposed here.

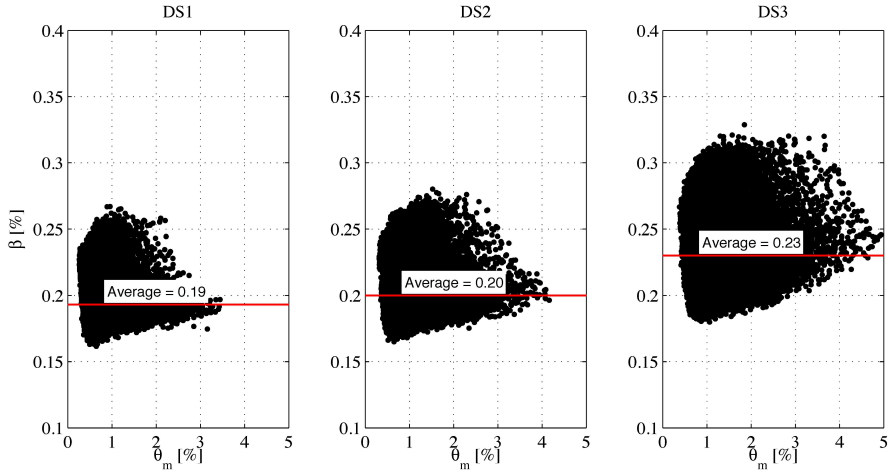

Figure 11: Observed β from the Monte Carlo Simulation of each damage state.

4.5 MATLAB Tool for Specific Case Fragility Function Generation

In addition to the storey based and general fragility functions outlined above, a MATLAB function is available which allows users to generate their own set of fragility functions for a given combination of link section, length and storey number. This tool functions by performing the MCS approach used in this study, but allows users to specify an exact combination of the three deterministic values, as opposed to general values such as those specified in Tables 3 and 4. The function performs the Lilliefors goodness-of-fit test to the simulated data as before and reports a set of median and dispersion values for each of the damage limit-states considered. In addition, should the user want to refine their interstorey drift-based fragility function set for a specific EBF structure, the MATLAB based tool provided allows for the user to specify all of the relevant parameters such as bay width, storey height, steel yield strength etc. in conjunction with the existing plastic chord rotation-based functions to result in an interstorey drift-based set of functions that have been directly converted to interstorey drift-based functions, given the users

inputs. This essentially means that the user has converted the fragility functions from a plastic chord rotation-based set to interstorey drift-based set instead of converting the interstorey drifts demands to plastic chord rotation demands to be input into PACT, which would create an additional EDP to track within the program. Further information and guidelines on how to implement the function are found at https://www.dropbox.com/s/ejkk5amr6r727ey/EBF_fragility.zip?dl=0.

4.6 Example Fragility Function Generation for a 5 Storey EBF

An example case study is examined to demonstrate the use of each of the four methods of establishing fragility function sets, depending on the availability of information and the required level of accuracy of the results. The example structure is to be taken as the fifth storey in a 10 storey EBF structure consisting of a HE220B link section with 600mm length and 7m bay width. Firstly, for the general set of functions presented in Section 4.2, these medians and dispersions are taken directly for the case study and reported in Table 5.

Table 5: Case study fragility curves.

Method	DS1		DS2		DS3	
	θ_c %	β	θ_c %	β	θ_c %	β
Generic	1.04	0.48	1.23	0.48	1.48	0.49
Storey Specific	0.95	0.32	1.16	0.35	1.44	0.40
Refined	0.71	0.19	0.84	0.20	1.01	0.23
MATLAB	0.75	0.18	0.89	0.20	1.05	0.23

For the storey number based set in Section 4.3, the set of functions corresponding to an *i* of 5 in Table 4 are selected. For the calculation of the median using Equation 11, the median values of the required variables are used and the median values are reported in Table 5. For the dispersion values of each of these damage states, the values reported in Figure 11 are adopted. For the MATLAB function method, the required input is used and the results included also in Table 5. A plot of each of these fragility function sets is presented in Figure 12 for each damage state. As can be seen, there is some degree of variability between the fragility function sets, depending on the level of detail input to obtain them where the more general fragility functions from Section 4.2 and 4.3 gave higher median interstorey drift and dispersion compared with the other two approaches in this case. Since the MATLAB function performs a MCS of the known scenario, this is taken to be the actual fragility function based on the results of this study. Figure 12 shows that the calculation of median drift capacities through Equation 11, and subsequently taking an assumed value of dispersion based on simulated data results, gave quite good results when compared with the result of the MATLAB function's exact scenario simulation.

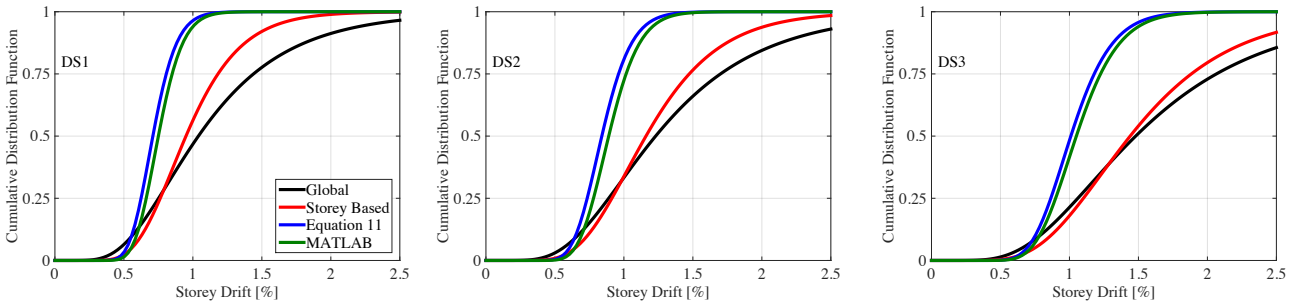

(a) DS1 **(b) DS2** **(c) DS3**

Figure 12: Case study fragility functions.

For cases when multi-bay EBF structures are being assessed with different bay lengths and link details, numerous sets of fragility functions will result, where the probability of each damage state will be computed for each bay using the bay's associated fragility function set for a given interstorey drift demand at a each floor. This applies to the case of the refined EBF fragility function outlined in Section 4.4 and the MATLAB based approach in Section 4.5. For the approaches outlined in Sections 4.2 and 4.3, the variability of bay length and link size has been accounted for through the epistemic uncertainty introduced during the Monte Carlo Simulation of the fragility functions, hence these general fragility function sets are valid for different bay lengths and link sizes. However, it is again highlighted that the fragility function sets developed in this article apply to EBFs with link elements placed in the centre of the bay, as illustrated in Figure 1.

5 Summary and Conclusions

The derivation of an interstorey drift-based fragility function set for EBF structures has been discussed. Analytical expressions for the determination of the yield drift of a given EBF configuration were reviewed and subsequently validated by comparing the results obtained from Equation 8 to those given by a series of pushovers of EBFs using an experimentally calibrated numerical model. Using the yield drift expression, a sensitivity study was conducted to determine the parameters most affecting the yield drift and ultimately, the drift capacity of an EBF system. This led to the determination of a set of parameters, which were identified to heavily influence the drift capacity of an EBF. A Monte Carlo Simulation (MCS) of this expression was conducted using a set of deterministic values and probabilistic distributions for the various influential variables. The resulting simulation led to the development of storey number based fragility function set, considering various link damage limit-states, a generic fragility function which does not require any knowledge of the EBF details, a storey-specific fragility function which is dependant only on the storey number, and a refined fragility function that is obtained using an expression to analytically derive median values to be used along with assumed values of dispersion. Lastly, a MATLAB code for specific fragility function set generation using the MCS process outlined to generate the previous two general sets is provided to allow computation of scenario specific fragility functions, should the user require such a level of refinement. As a result of this study, the following conclusions are drawn:

- An interstorey drift-based fragility function has been established for EBFs, which identifies three different link damage limit-states reported from experimental testing. This

leads to a more direct assessment of damage, and subsequently losses, for an EBF structure when carrying out a probabilistic loss assessment of an EBF structure.

- Should more detailed information be available regarding the EBF structure, a set of fragility functions can be established by first determining the median values for each damage state, followed by an assumption of the associated dispersion based on previous MCS results. A case study example demonstrated that this approach was the most accurate at determining the median values of interstorey drift capacity when compared with MCS results in addition to having a reduced dispersion compared to the more general fragility function sets.
- A MATLAB based fragility function tool has been developed that allows users to generate a more refined set of fragility functions corresponding to the damage limit-states outlined in Section 4 by performing a Monte Carlo Simulation of the user defined parameters for the EBF. This essentially means that the user has converted the fragility functions from a plastic chord rotation-based set to interstorey drift-based set instead of converting the interstorey drifts demands to plastic chord rotation demands.

In addition to providing a set of fragility functions that can be used for performance assessment, these fragility functions can be used to determine the likelihood that a given link in an EBF structure has exceeded a certain damage state and requires repair. This could be particularly useful when considering the observations of Clifton *et al.* (2011) during reconnaissance inspections of EBF structures following the 2010 and 2011 Canterbury earthquakes in New Zealand, where it was reported that architectural and floor finishes inhibited proper inspection of the links following the event. However, a set of fragility functions such as those developed in this paper could be used to determine the likelihood of damage and justify the need for intervention and full structural inspection should information on the maximum interstorey drift be available.

References

AISC 341-10. 2010. "Seismic Provisions for Structural Steel Buildings." AISC 341-10. Chicago, Illinois, USA.

Ang, A., and W. Tang. 2007. *Probability Concepts in Engineering, Emphasis on Applications in Civil and Environmental Engineering*. John Wiley & Sons, Ltd.

Arce, G. 2002. "Impact of Higher Strength Steels on Local Buckling and Overstrength of Links in Eccentrically Braced Frames.", MSc Thesis, The University of Texas at Austin.

Braconi, A., M. Badalassi, and W. Salvatore. 2010. "Modeling of European Steel Qualities Mechanical Properties Scattering and Its Influence on Eurocode 8 Design Requirements." In *14ECEE - European Conference on Earthquake Engineering*. Vol. 1998. Ohrid, Macedonia.

Clifton, C., M. Bruneau, G. A. MacRae, R. Leon, and A. Fussell. 2011. "Steel Structures Damage from the Christchurch Earthquake Series of 2010 and 2011." *Bulletin of the New Zealand Society for Earthquake Engineering* 44 (4): 297–318.

Corus. 2006. "Structural Sections to BS4: Part 1: 1993 and BS EN10056: 1999." North Lincolnshire, U.K.

CSA S16-09. 2009. "Design Of Steel Structures." CSA S16-09. Vol. 8523. Ontario, Canada.

Della Corte, G., M. D'Aniello, and R. Landolfo. 2013. "Analytical and Numerical Study of Plastic Overstrength of Shear Links." *Journal of Constructional Steel Research* 82 (March): 19–32. doi:10.1016/j.jcsr.2012.11.013.

EN 1993-1-1:2005. 2005. "Eurocode 3: Design of Steel Structures - Part 1-1: General Rules and Rules for Buildings." EN 1993-1-1:2005. Brussels, Belgium.

EN 1998-1:2004. 2004. "Eurocode 8: Design of Structures for Earthquake Resistance - Part 1: General Rules, Seismic Actions and Rules for Buildings." Comité Européen de Normalisation. Brussels, Belgium.

Engelhardt, M. D., and E. P. Popov. 1989. "Behavior of Long Links in Eccentrically Braced Frames." Research Report UCB/EERC-89/01. Berkeley, California.

FEMA P58-1. 2012. "Seismic Performance Assessment of Buildings: Volume 1 - Methodology (P-58-1)." Vol. 1. Washington, DC.

FEMA P58-2. 2012. "Seismic Performance Assessment of Buildings: Volume 2 - Implementation Guide (P-58-2)." Vol. 2. Washington, DC.

Galvez, P. 2004. "Investigation of Factors Affecting Web Fractures in Shear Links.", MSc Thesis, The University of Texas at Austin.

Gulec, C. K., B. Gibbons, A. Chen, and A. S. Whittaker. 2011. "Damage States and Fragility Functions for Link Beams in Eccentrically Braced Frames." *Journal of Constructional Steel Research* 67 (9) (September): 1299–1309. doi:10.1016/j.jcsr.2011.03.014. http://linkinghub.elsevier.com/retrieve/pii/S0143974X11000800.

Kuşyilmaz, Ahmet, and Cem Topkaya. 2015. "Displacement Amplification Factors for Steel Eccentrically Braced Frames." *Earthquake Engineering & Structural Dynamics* 44 (2) (February): 167–184. doi:10.1002/eqe.2463. http://doi.wiley.com/10.1002/eqe.2463.

Mansour, N. 2010. "Development of the Design of Eccentrically Braced Frames with Replaceable Shear Links." PhD Thesis, Department of Civil Engineering, University of Toronto.

MATLAB. 2014. *Version 8.3.0 (R2014a)*. Natick, Massachusetts: The Mathworks Inc.

Mazzolani, F. M., R. Landolfo, G. Della Corte, and B. Faggiano. 2006. "Edifici Con Struttura Di Acciaio in Zona Sismica." (in Italian) IUSS Press, Pavia, Italy.

McKenna, F., G. Fenves, F. C. Filippou, and S. Mazzoni. 2000. "Open System for Earthquake Engineering Simulation (OpenSees)." http://opensees.berkeley.edu/wiki/index.php/Main_Page.

NZS 3404. 2007. "Steel Structures Standard." NZS 3404:Part 1:1997. Wellington, New Zealand.

O'Reilly, Gerard J., and Timothy J. Sullivan. 2015. "Direct Displacement-Based Seismic Design of Eccentrically Braced Steel Frames." *Journal of Earthquake Engineering* (September 4). doi:10.1080/13632469.2015.1061465. http://www.tandfonline.com/doi/full/10.1080/13632469.2015.1061465.

Okazaki, T., G. Arce, H. C. Ryu, and M. D. Engelhardt. 2005. "Experimental Study of Local Buckling, Overstrength, and Fracture of Links in Eccentrically Braced Frames." *Journal of Structural Engineering* 131 (10) (October 1): 1526–1535. doi:10.1061/(ASCE)0733-9445(2005)131:10(1526).

Okazaki, T., and M. D. Engelhardt. 2007. "Cyclic Loading Behavior of EBF Links Constructed of ASTM A992 Steel." *Journal of Constructional Steel Research* 63 (6) (June): 751–765. doi:10.1016/j.jcsr.2006.08.004.

Okazaki, T., M. D. Engelhardt, A. Drolias, E. Schell, J. K. Hong, and C. M. Uang. 2009. "Experimental Investigation of Link-to-Column Connections in Eccentrically Braced Frames." *Journal of Constructional Steel Research* 65 (7) (July): 1401–1412. doi:10.1016/j.jcsr.2009.02.003.

Porter, K. A. 2003. "An Overview of PEER's Performance-Based Earthquake Engineering Methodology." In *Proceedings of Ninth International Conference on Applications of Probability and Statistics in Engineering*. Vol. 8. San Francisco, CA.

Porter, K. A., J. L. Beck, and R. V. Shaikhutdinov. 2004. "Simplified Estimation of Economic Seismic Risk for Buildings." *Earthquake Spectra* 20 (4) (November): 1239–1263. doi:10.1193/1.1809129. http://earthquakespectra.org/doi/abs/10.1193/1.1809129.

Richards, P. W., and C. M. Uang. 2006. "Testing Protocol for Short Links in Eccentrically Braced Frames." *Journal of Structural Engineering* 132 (8) (August 1): 1183–1191. doi:10.1061/(ASCE)0733-9445(2006)132:8(1183).

Rossi, P.P., and A. Lombardo. 2007. "Influence of the Link Overstrength Factor on the Seismic Behaviour of Eccentrically Braced Frames." *Journal of Constructional Steel Research* 63 (11) (November): 1529–1545. doi:10.1016/j.jcsr.2007.01.006. http://www.sciencedirect.com/science/article/pii/S0143974X07000119.

Ryu, H. C. 2005. "Effects of Loading History on the Behavior of Links in Seismic-Resistant Eccentrically Braced Frames.", MSc Thesis, The University of Texas at Austin.

Sullivan, T. J. 2013. "Direct Displacement-Based Seismic Design of Steel Eccentrically Braced Frame Structures." *Bulletin of Earthquake Engineering* 11 (6) (July 13): 2197–2231. doi:10.1007/s10518-013-9486-8.

Uriz, P., and S. A. Mahin. 2008. "Toward Earthquake-Resistant Design of Concentrically Braced Steel-Frame Structures." PEER Report No. 2008/08. Berkeley, California.

Welch, D. P., T. J. Sullivan, and G. M. Calvi. 2014. "Developing Direct Displacement-Based Procedures for Simplified Loss Assessment in Performance-Based Earthquake Engineering." *Journal of Earthquake Engineering* 18 (2) (February 17): 290–322. doi:10.1080/13632469.2013.851046.